applied sciences

MDPI

Review

An Insight into the Chemistry of Cement—A Review

Luca Lavagna [1,*] and Roberto Nisticò [2,*]

[1] Department of Applied Science and Technology, Politecnico di Torino, C.so Duca degli Abruzzi 24, 10129 Torino, Italy
[2] Department of Materials Science, University of Milano-Bicocca, INSTM, Via R. Cozzi 55, 20125 Milano, Italy
* Correspondence: luca.lavagna@polito.it (L.L.); roberto.nistico@unimib.it (R.N.)

Abstract: Even if cement is a well-consolidated material, the chemistry of cement (and the chemistry inside cement) remains very complex and still non-obvious. What is sure is that the hydration mechanism plays a pivotal role in the development of cements with specific final chemical compositions, mechanical properties, and porosities. This document provides a survey of the chemistry behind such inorganic material. The text has been organized into five parts describing: (i) the manufacture process of Portland cement, (ii) the chemical composition and hydration reactions involving a Portland cement, (iii) the mechanisms of setting, (iv) the classification of the different types of porosities available in a cement, with particular attention given to the role of water in driving the formation of pores, and (v) the recent findings on the use of recycled waste materials in cementitious matrices, with a particular focus on the sustainable development of cementitious formulations. From this study, the influence of water on the main relevant chemical transformations occurring in cement clearly emerged, with the formation of specific intermediates/products that might affect the final chemical composition of cements. Within the text, a clear distinction between setting and hardening has been provided. The physical/structural role of water in influencing the porosities in cements has been analyzed, making a correlation between types of bound water and porosities. Lastly, some considerations on the recent trends in the sustainable reuse of waste materials to form "green" cementitious composites has been discussed and future considerations proposed.

Keywords: ceramic materials; composites; inorganic materials; oxides; Portland cement; porous materials

Citation: Lavagna, L.; Nisticò, R. An Insight into the Chemistry of Cement—A Review. *Appl. Sci.* **2023**, *13*, 203. https://doi.org/10.3390/app13010203

Academic Editors: Mariella Diaferio and Francisco B. Varona Moya

Received: 23 November 2022
Revised: 15 December 2022
Accepted: 21 December 2022
Published: 23 December 2022

1. Introduction

Cement is a hydraulic binder; it consists of a finely ground inorganic material which forms a paste when mixed with water, is able to set and harden because of numerous exothermic hydration reactions (and processes), and is thus capable of binding fragments of solid matter to form a compact whole solid [1–3]. After hardening, cement retains its strength and stability, even under the effect of water. Cement forms a composite defined as mortar when mixed with water and fine aggregate (i.e., sand), whereas it forms concrete when mixed with water, sand and gravel (i.e., small stones) [4]. Cement-based materials, such as concrete, have been used for many centuries, mostly in the construction and civil engineering fields, thus becoming the most widely used material, and the second most consumed resource on Earth [5]. Among the different types of cement, ordinary Portland cement (OPC) is the most widely used one [6].

Even if the technology of cement seems quite well established, recent discoveries in nanotechnology and materials science (e.g., the discovery of graphene) opened the possibility of inducing novel smart functionalities in cement and concrete, allowing their use in advanced technological applications. Examples of such systems are self-healing systems [7,8], health-monitoring systems [9,10], conductive materials [11], water permeable

materials [12], thermal energy storage materials [13], rubberized concrete [14–17], and sustainable composites containing bio-based fillers [18–20].

From the economic viewpoint, even if cement-based materials are low-cost products (with a maximum cost of 155 EUR ton^{-1}), cements still represent raw materials of remarkable interest for the global market (i.e., cement accounted for 0.074% of total world trade in 2020). Countries leading in the worldwide exportation of cement in 2020 were Vietnam (USD 1.5 billion, covering almost 12% of the global market), Turkey (USD 1.3 billion, 10.3%), United Arab Emirates (USD 578 million, 4.7%), Thailand (USD 574 million, 4.6%), and Germany (USD 528 million, 4.3%) [21]. On the other hand, the largest global importers of cement-based materials are the US (USD 2.3 billion, 10.5%), China (USD 1.2 billion, 9.7%), Bangladesh (USD 513 million, 4.1%), Philippines (USD 464 million, 3.7%), and France (USD 452 million, 3.7%) [21].

This document aims to provide a useful survey of the chemistry behind cement and cement-based materials. Particular attention has been dedicated to the key role played by water in the hydration reactions occurring in OPC, and the different types of compounds generated during this step. In this context, the recent literature [22–41] clearly highlights the pivotal interest still present in the development of new advanced cement and cementitious materials. Even if cement is a well-consolidated material, the chemistry of cement (and the chemistry inside cement) remains very complex and not obvious. Therefore, in this study, the different chemical compounds generated during hydration and setting are clearly investigated, keeping an eye on their mechanisms of formation. Furthermore, the physical and structural role of water in driving the entire process of pores formation has been considered. Lastly, a dedicated section regarding the latest developments in the field of sustainable recycling for the construction industry has been proposed, with a special focus on the use of recycled (waste) materials to produce a new generation of "green" concretes and mortars.

2. The Manufacture of OPC

OPC is a fine grey/white powder consisting of a mixture of calcium silicates, aluminates, and aluminoferrites. These raw materials can be classified into four distinct groups: calcareous, siliceous, argillaceous, and ferriferous. Such raw materials are thermally treated via pyrolysis and mechanically processed in order to obtain the desired product with specific compositions and defined mechanical properties. Cement manufacturing implies four different steps: quarrying, raw material preparation, clinkering, and cement preparation [42]. Figure 1 schematically represents the production line of an OPC [43]. The entire production process begins with the extraction of the previously described raw materials that are rock mixes mainly constituted by ca. 80% of limestone (i.e., primarily calcium carbonate mineral $CaCO_3$) and 20% of either clays or shale (i.e., a source of silica SiO_2, alumina Al_2O_3, and hematite Fe_2O_3) [44].

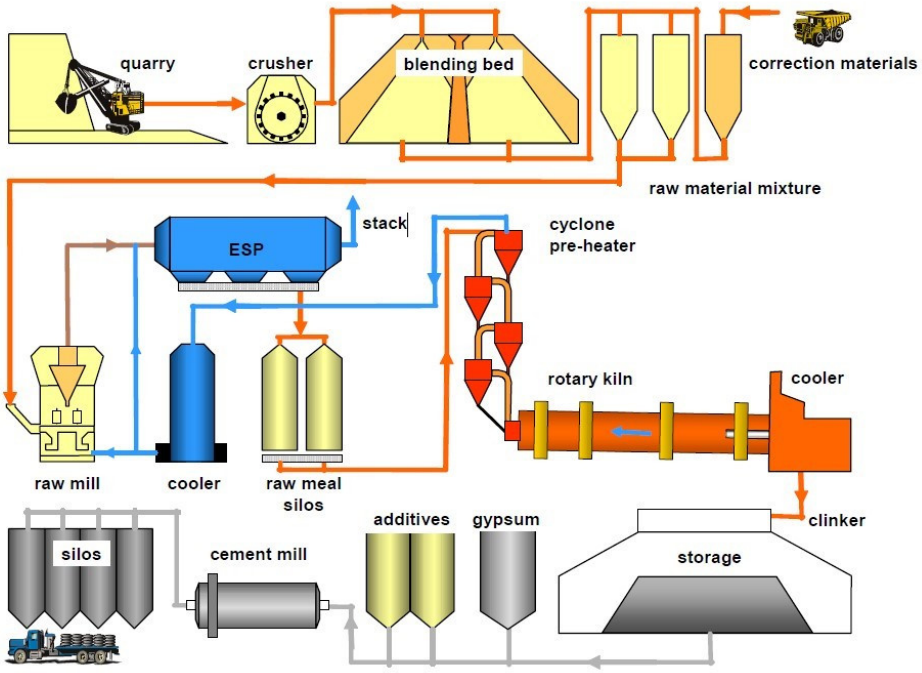

Figure 1. Schematic representation of the process of cement manufacturing. Reprinted with permission from [43].

Once raw materials are extracted, they are pre-crushed inside a quarry. Subsequently, crushed raw material is prepared by applying a variety of blending and sizing operations to confer appropriate chemical and physical properties to the feed. These processing steps can be divided into two different approaches, namely, either dry or wet. Concerning the dry route, both limestone and clays are independently crushed, and then fed together inside a mill. The wet route, instead, requires clays to be mixed forming a paste inside a wash mill (i.e., a tank where clays are grinded in the presence of water), and crushed limestone is added only at the end. Finely ground materials are dried, thermally treated inside a kiln, and then cooled down. This series of steps is defined as clinkering and it confers the main relevant features of the OPC manufacturing. In fact, clinkering reshapes the starting raw materials mixture into clinkers, which are grey, spherically shaped nodules whose diameter is 5–25 mm in size [45]. The chemical reactions occurring inside the kiln, kept heated by the spontaneous ignition of the pulverized coal dusts introduced inside the system due to the high temperatures, is still not completely understood. These chemical reactions are influenced by several factors, such as the large variety in terms of starting chemical compositions, the operating parameters of processing, and the difficulties in performing an efficient in situ sampling under the processing conditions (i.e., high temperatures). However, the chemical reactions and physical processes involved in this step can be rationalized as follow:

1. Evaporation of the physically sorbed water molecules from the raw mix (20–100 °C).
2. Dehydration (100–430 °C) with the production of oxides, such as silica, alumina, and hematite.
3. Calcination (800–1100 °C) with the development of calcium oxide, according to the carbonate decomposition reaction:
   $CaCO_3 \rightarrow CaO + CO_2$
4. Exothermic reactions (1100–1300 °C) with the formation of secondary silicate phases:
   $2CaO + SiO_2 \rightarrow 2CaO \cdot SiO_2$
5. Sintering and reactions occurring inside the melt (1300–1450 °C) with conversion of secondary silicate phases into both ternary silicates and tetracalcium aluminoferrites:
   $2CaO \cdot SiO_2 + CaO \rightarrow 3CaO \cdot SiO_2$

$3CaO \cdot Al_2O_3 + CaO + Fe_2O_3 \rightarrow 4CaO \cdot Al_2O_3 \cdot Fe_2O_3$

6. Cooling of the system, and the crystallization of the other mineral phases.

Finally, the resulting clinker is further united with gypsum and then ground. From the energetic viewpoint, the grinding process consumes ca. 60% of the total electrical energy involved in a standard cement plant (high cost). In a conventional cement making process, the electrical energy consumed is 4approx. 110 kWh/tons, with ca. 30% used for raw material preparation and ca. 40% for the grinding step. The resulting cement is pneumatically pumped toward specific silos for storage and is subsequently drawn either for packing inside paper bags or for storage inside bulk vessels [46].

3. Hydration Step Involving OPC

Hydration refers to chemical reactions between anhydrous compounds with water molecules, giving a plethora of hydrated compounds. The hydration phenomenon occurring in cement consists of the chemical reaction between non-hydrated cement and water that allows for important physicochemical transformations and mechanical changes. In this context, a distinction should be made between the partial hydration by means of the moisture contained in an air atmosphere, and the hydration achieved by the direct mixing of the cement with water [47]. In this last case (i.e., direct mixing), several chemical reactions take place, inducing the conversion from a workable paste with plastic features to a hard solid. Furthermore, since the hydration of OPC consists of a multitude of simultaneous single chemical reactions involving the different main components forming the cement powder with water, the resulting pathway is rather complex and non-obvious, and its degree of complexity is strongly influenced by the starting composition of the clinker that directly affects the transformation occurring within the cementitious matrices.

3.1. Typical Starting Composition of Cement and Mineral Phases

The starting composition of clinker is generally indicated by the oxide content (in wt.%). The main relevant oxides forming an OPC clinker are CaO, SiO_2, Al_2O_3 and Fe_2O_3. These oxides form different mineral phases when forming the clinker. Since clinker primarily contains these four chemical species, it is possible to represent these phases with the Bogue formulae, thus indicating CaO with C, Al_2O_3 with A, Fe_2O_3 with F, SiO_2 with S, and water with H [26]. Furthermore, there are also several further minor components deriving from natural clays, e.g., sodium (Na), potassium (K), magnesium (Mg), and other metal ions [48,49]. Table 1 summarizes the chemical composition of OPC, expressing the single component content in wt.%. Additionally, Table 2 describes the approximate composition of the cement clinker [50].

Table 1. Main components of an OPC.

Compounds	Chemical Formula	Bogue Formula	Amount (wt.%)
Alite, or Tricalcium silicate	Ca_3SiO_5 $[3CaO \cdot SiO_2]$	C_3S	30-50
Belite, or Dicalcium silicate	Ca_2SiO_4 $[2CaO \cdot SiO_2]$	C_2S	20-45
Celite, or Tricalcium aluminate	$Ca_3Al_2O_6$ $[3CaO \cdot Al_2O_3]$	C_3A	8-12
Brownmillerite, or Tetracalcium aluminoferrite	$Ca_4Al_2Fe_2O_{10}$ $[4CaO \cdot Al_2O_3 \cdot Fe_2O_3]$	C_4AF	6-10
Gypsum, or Calcium sulphate dihydrated	$CaSO_4 \cdot 2H_2O$	-	4-8
Potassium oxide	K_2O	K	<2
Sodium oxide	Na_2O	N	<2

Table 2. Chemical composition of OPC clinkers.

Component	Amount (wt.%)
CaO	58.0-68.0
SiO_2	16.0-26.0
Al_2O_3	4.0-8.0
Fe_2O_3	2.0-5.0
MgO	1.0-4.0
SO_3	0.1-2.5

3.2. Chemical Reactions Occurring during the Hydration Process

A series of separate/independent (parallel and/or sequential) reactions involving water molecules and the principal mineral phases forming the cement led to the hydration of OPC. In general, the hydration process is strongly driven by the starting chemical composition, the dimensions and size (e.g., specific surface areas, roughness, and particle size distribution), the quantity of water added, the water-to-cement ratio (*w*/*c*), the curing temperature, and the presence of additives [51]. In order to simplify the comprehension of the process, the following hydration reactions are discussed separately by considering minerals individually. Figure 2 reports the principal hydrated products in OPC [52].

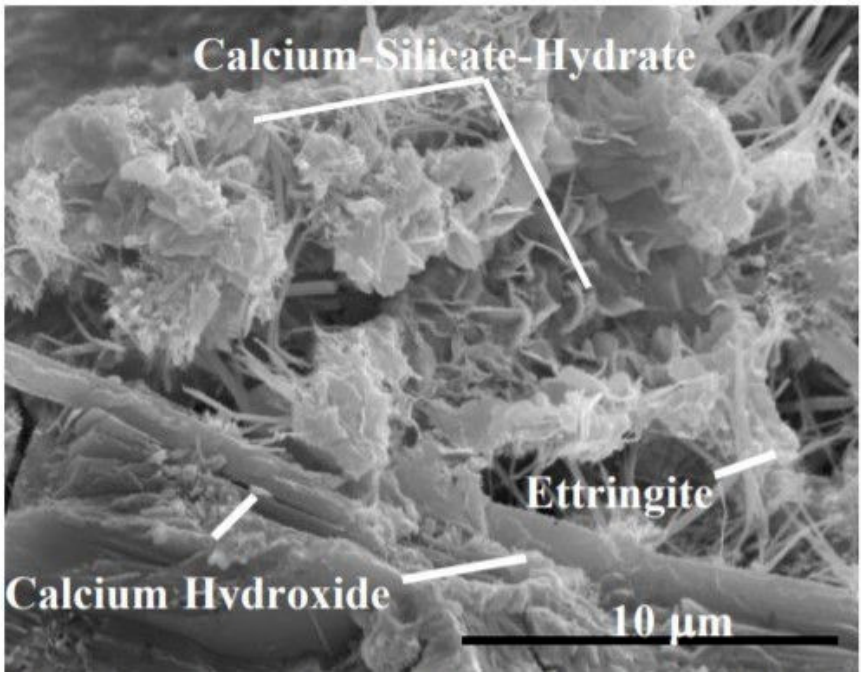

Figure 2. SEM micrograph of the fracture surface of hardened OPC paste after seven days of hydration. Reprinted with permission from [52].

3.2.1. Reaction Involving C_3S

The principal constituent of the OPC is the tricalcium silicate (C_3S, or alite). Alite largely affects the cement mechanical properties (strength) and the hardening process. During the alite hydration, four stages may be distinguished. The first one is the pre-induction period (duration time: a few minutes, just after being exposed to water) where the rapid hydration of C_3S occurs. When C_3S is exposed to water, at the surface level, ions start to a rapidly dissolve, with release of hydroxyl and silicate ions in the liquid phase. As a result, the positive charge of Ca^{2+} is counterbalanced by the negative ones due to silicate and hydroxyl anions. Since the dissolution rate of C_3S is faster than the diffusion rate of ions at the surface level, the liquid phase rapidly turns oversaturated considering the silicate hydrated phase. The direct consequence of this phenomenon is the precipitation of a first layer of C-S-H (i.e., tobermorite) nearby the surface. A high heat of hydration

is produced in this first step of reaction [53]. Immediately after, the rate of hydration slows down and then increases, with a second heat release. Finally, the hydration process slows down again, entering the deceleration step [54]. The explanation of this specific behavior is the object of several theories, and some considerations regarding kinetic aspects are reported in the literature [55].

C-S-H is the main relevant binding phase, and is chemically defined as $CaO \cdot SiO_2 \cdot H_2O$. The stoichiometry of C-S-H in the cement paste is variable (and this is particularly true for the bound water). Additionally, a secondary product, calcium hydroxide or portlandite (i.e., $Ca(OH)_2$, or CH), is generated in the case of a CaO/SiO_2 molar ratio which is smaller than the alite one (namely, 3:1).

3.2.2. Reaction Involving C_2S

In analogy with the previously described alite, the hydration of dicalcium silicate (C_2S, or belite) also requires different reaction steps. In general, the induction time is significant, with a low hydration rate. Then, a second slight increment in the hydration rate occurs. Finally, the hydration rate reduces again in the third step. Belite evolves into both C-S-H and CH [56].

3.2.3. Reaction Involving C_3A

Tricalcium aluminate (C_3A, or celite), the most reactive component present in cement, is the third species involved in the hydration mechanism. Its role in the first step of hydration is of paramount relevance as it influences both the mechanical and rheological properties. Furthermore, gypsum can determine the chemistry of the products obtainable through the hydration of celite. Without gypsum, the formation of a gel-like material can be registered at the surface of cement as the first hydration product. Proceeding with the hydration, this material transforms itself into hexagonal crystals of C_2AH_8 and C_4AH_{13} (or C_4AH_{19}). These products convert into cubic C_3AH_6. It is important to note that both C_2AH_8 and C_4AH_{19} are metastable products, whereas the cubic C_3AH_6 is the calcium aluminate hydrate form stable at RT [57]. The fast precipitation of hexagonal platelets causes the phenomenon defined as "flash set". A high temperature of hydration corresponds with a high rate of conversion towards the most stable hydration products. Additionally, at temperatures higher than 80°C, C_3AH_6 directly forms from the hydration of C_3A. Both C_2AH_8 and C_4AH_{19} are considered as Afm, which indicates a subfamily of mono-hydrated calcium aluminate phases structurally related to hydrocalumite, with the representative formula of $[Ca_2(Al,Fe)(OH)_6] \cdot X \cdot xH_2O$, where X corresponds to an exchangeable anion.

To prevent the fast setting of the paste, and elongate the period of workability, gypsum is usually added to the clinker. With gypsum, the principal hydration phase is ettringite (or $C_6AS_3H_{32}$), which belongs to the Aft group, which indicates a subfamily of three-hydrated calcium aluminate phases with the representative formula $[Ca_3(Al,Fe)(OH)_6] \cdot X_3 \cdot xH_2O$, where X equals a doubly charged anion [58,59]. If sulfate ions are available in the system, the ettringite phase remains stable. When gypsum is fully consumed, ettringite chemically reacts with further C_3A, forming Afm. The gradual consumption of ettringite, instead, favors the growth of hexagonal calcium aluminate hydrate, C_4AH_{13} [60].

3.2.4. Reaction Involving C_4AF

The last component that participates in the hydration reaction is calcium aluminoferrite (C_4AF, or brownmillerite). This compound is the only variable phase present in cement with an unfixed composition. Brownmillerite constitutes a wide category of solid solution $Ca_2(Al_yFe_{(2-y)})O_5$, where the values of y are in the 0.00–1.33 range. Analogous to the previous component C_3A, the hydration of C_4AF is affected by the presence/absence of gypsum. The absence of gypsum favors the reaction of C_4AF with water, forming metastable C(A,F)H hydrates (defined as hydroxy-Afm phase) onto the surface of the non-

hydrated grains, and eventually the stable phase $C_3(A,F)H_6$. Experimentally, it has been demonstrated that the Al^{3+}/Fe^{3+} ratio is usually lower in the products formed by the reaction with water with respect to the original C_4AF [61]. The reduction in Al^{3+}/Fe^{3+} in the hydrated products can be clarified by means of the production of a secondary by-product, namely, an amorphous iron-rich gel or iron hydroxide [62].

Conversely, in the presence of gypsum, C_4AF produces hydration phases analogous to the case of C_3A. However, the reaction rates of both components are quite different. In fact, in the presence of gypsum, C_4AF reacts much slower than C_3A, i.e., gypsum retards the hydration of C_4AF more efficiently than in the case of C_3A. However, the rate of hydration of C_4AF is affected by the composition of the ferrite phase: the high amount of Fe corresponds to a low rate of hydration [63]. Therefore, gypsum favors the AFt phase as the main product of reaction, whereas in a successive reaction step, the AFt phase evolves into AFm by reaction with further C_4AF.

3.3. Mechanism and Heat of Hydration of OPC

The kinetics of hydration defines both the cement microstructure and its final properties. The cement–water reaction causes both the dissolution of the anhydrous phases and the precipitation of the hydrated ones. Hence, its evolution with time is subject to the kinetics of dissolution [64], and the growth of the hydrated crystals with their rate of nucleation [65]. Figure 3 reports the kinetics of hydration for an OPC [1]. The hydration process of cement can be organized into four stages: pre-induction, induction (dormant), acceleration, and a post-acceleration period. Every step is discussed in the following paragraphs [66].

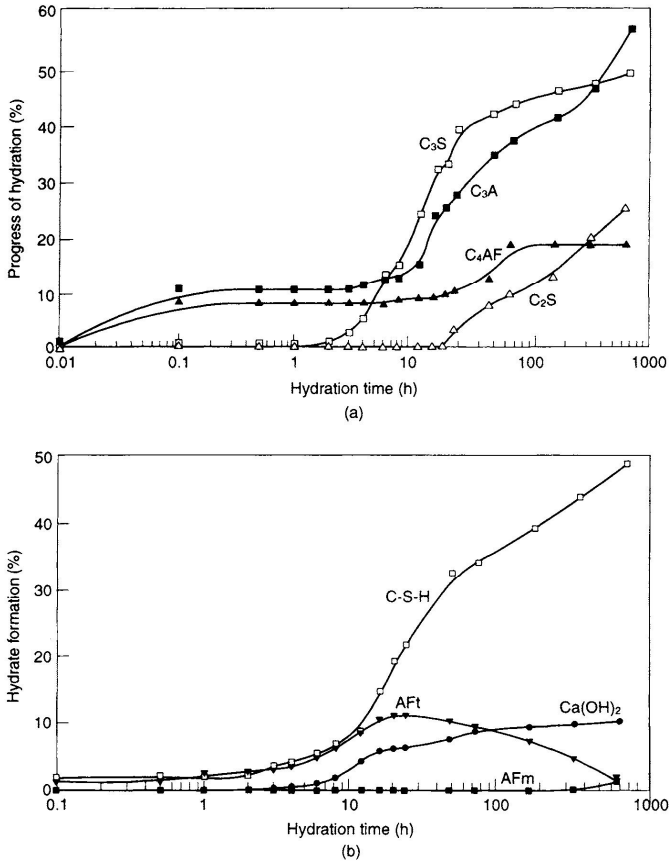

Figure 3. Graph reporting the progress of hydration as a function of the hydration time for the principal components of an OPC: consumption of clinker phases ((**a**), top), and formation of hydrate phases ((**b**), bottom). Reprinted with permission from [1].

3.3.1. Pre-Induction Period

Once cement interacts with water, ionic species rapidly go in the solution allowing the formation of hydrates. From the dissolution of alkali sulphates, there is the release of free potassium, sodium, and sulphate ions. Gypsum dissolves until saturation, releasing Ca^{2+} and SO_4^{2-}.

The literature evidences the creation of a coating growing over the surface of the cement grains immediately after contact with water [67,68]. This product is recognized as being C-S-H. The layer of C-S-H grows, covering most of the grain surface, until the exhaustion of reactants available at the surface. According to Thomas et al. [69], when the content in the C_3S product is higher than the CaO/SiO_2 ratio, during this first step of hydration, there is an increment in the concentration of Ca^{2+} and OH^- in the liquid. Furthermore, adding water to the cement leads to the rapid dissolution of both gypsum and clinker minerals, producing Ca^{2+}, OH^-, SO_4^{2-} ions, and ionic concentration differences through steps in the liquid phase, and causing the supersaturation phenomenon necessary for the formation of the ettringite phase.

Moreover, Jiahui et al. [70] pointed out that the formation of octahedral $[Al(OH)_6]^{3-}$ is the time-determining step in controlling the AFt growth. Furthermore, it has been demonstrated that the ionic concentration affects the kinetic rate of the reaction. Among the different ions forming ettringite, $[AlO_2]^-$ is the one with the lowest concentrated one, and is consequently the limiting species. There are only a small quantity of C_2S hydrates within this first step. Furthermore, the belite (i.e., C_2S) reaction rate is similar, but slower, in respect to that of C_3S, and this is probably attributable to both belite's high thermodynamic stability in respect to alite, and its different crystalline structure. Lastly, C_2S presents high density, and the presence of holes/pores/channels in the structure of C_3S facilitates the reaction with water [71].

3.3.2. Induction (Dormant) Period

After the fast hydration step of cement, the general hydration rate slows down for some hours. The explanation of this sharp slowdown is probably attributable to two main theories, considering both the apparent low reactivity of C_3S and its high solubility calculated from the enthalpy of formation. The first theory is named as the theory of the protective membrane, and it considers the decrease in the hydration rate attributable to the formation of metastable C-S-H layers covering the reacting surface of cement particles, thus preventing the fast dissolution ability of C_3S [72]. Several studies reported in the literature evidenced the tendency of C-S-H to rapidly form once it has interacted with water [73]. In principle, the formation of a low-permeable layer of hydrates, with enough density and coverage, should be able to slow down the ion diffusion rate from the anhydrous cement grains. However, experimental evidence confirms that C-S-H does not form a continuous layer around the grains. In this way, there is still contact with the pore solution, thus weakening this theory [74].

The second theory, the theory of dissolution, instead suggests that the slowdown rate is principally due to the decrease in the kinetic of dissolution of both C-S-H and alite when the system is evolving towards the equilibrium condition. In this context, it should be highlighted that the dissolution of C_3S has been mostly simplistically considered in all models addressing the hydration kinetics of cementitious matrices. This is probably caused by the dissolution step, which in most cases has been studied independently from the other mechanisms that characterize the hydration step. As dissolution occurs together with the precipitation of hydrate phases at the surface, this might interfere with the dissolution process involving the cement components. Hence, this theory remains valid, but the role of the kinetics of dissolution should be highlighted [75].

3.3.3. Acceleration Period

During this step, hydration accelerates once again. The C_3S hydration favors the formation of the "outer" C-S-H, which is different from the "inner" C-S-H. Tennis et al. [76] proposed a model describing the formation of calcium silicate hydrate, making a distinction between low-density (LD) C-S-H ("outer" product), and high-density (HD) C-S-H ("inner" product). Figure 4 shows a C_3S grain after 96 h of hydration, where both C-S-H products are present [77]. In particular, the "outer" C-S-H forms during the early hydration step. It is easily recognizable as it remains away from the cement particle surface, and it is highly porous. On the other hand, the "inner" C-S-H forms during the late hydration step, and it has low porosity. Furthermore, the amount of "inner" C-S-H increases as the *w*/*c* ratio decreases [78].

During this step, a noticeable hydration of C_2S is also registered. Moreover, Portlandite (i.e., CH) precipitates from the liquid, thus decreasing the amount of Ca^{2+} ions in the liquid. Gypsum, instead, completely dissolves. Quite surprisingly, the concentration of SO_4^{2-} anions in the liquid decreases, probably because of the occurrence of two phenomena: (i) the formation of the AFt phase, and (ii) the adsorption of SO_4^{2-} ions at the surface of the C-S-H phase.

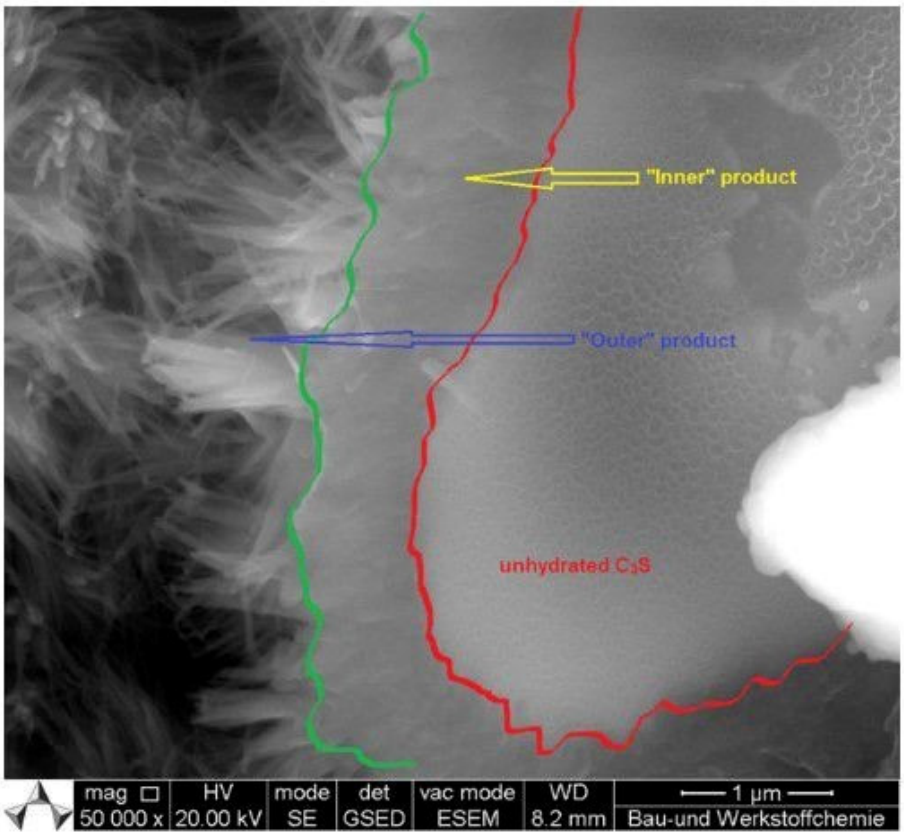

Figure 4. SEM micrograph showing the two types of C-S-H produced during hydration; namely, the "outer" product away from the cement particle surface, occupying the water-filled space and characterized by high porosity, and the "inner" C-S-H formed during later steps of hydration and characterized by low porosity. Reprinted with permission from [77].

3.3.4. Post-Acceleration Period

During this step, the hydration rate decelerates, and the "inner" C-S-H starts forming from hydration reactions involving both C_3S and C_2S. According to Bazzoni et al. [79], the

acceleration period involves the nucleation (and growth) of C-S-H clusters onto the surfaces of the cement grains. The deceleration period, instead, involves a substantial decrease in the growth rate of C-S-H that, at this point of the process, covers much of the grains surface. In fact, this final period of hydration involves a low hydration rate, probably caused by the less available space. In particular, the formation of hydrates occurs only in space filled with water. Such a lack of available space is attributable to two phenomena: (i) the depletion of the water volume (necessary for hydrates' precipitation), and (ii) the sequestration of the remaining water into pores whose critical pore sizes are smaller for precipitation [80].

Moreover, together with the formation of "inner" C-S-H, there is a continuous consumption of gypsum, until it is fully consumed. In this way, the concentration of the sulphate ions in the liquid decreases, and the AFt phase (produced during the earlier steps of hydration) begins to chemically react with further C_3A and $C_2(A,F)$, thus forming the AFm phase [81].

3.3.5. Consideration over the Heat of Hydration

Figure 5 reports the heat of hydration of an OPC over the hydration time [1]. The curve profile evidences six different thermal phenomena. The first one is an initial sharp endothermic peak soon after mixing, probably due to the dissolution of potassium sulphate in water (i.e., this contribution is present only in cement containing potassium sulphate, as seen in Figure 5, step 1). The second one is an intense exothermic peak (with a maximum centered in the very first minutes) attributable to the initial hydration reactions involving C_3S, C_3A, and gypsum (Figure 5, step 2). The third one corresponds to the induction (dormant) period, and it is associated with a minimum of the heat of hydration (Figure 5, step 3). The fourth one is an intense exothermic peak attributable to the hydration of C_3S and the consequent conversion into C-S-H and CH (Figure 5, step 4). The fifth one corresponds to a small descending branch of the principal peak, probably attributable to the AFt formation (Figure 5, step 5), whereas the sixth one corresponds to another small descending branch of the principal peak attributable to the Aft–AFm conversion (Figure 5, step 6) [1].

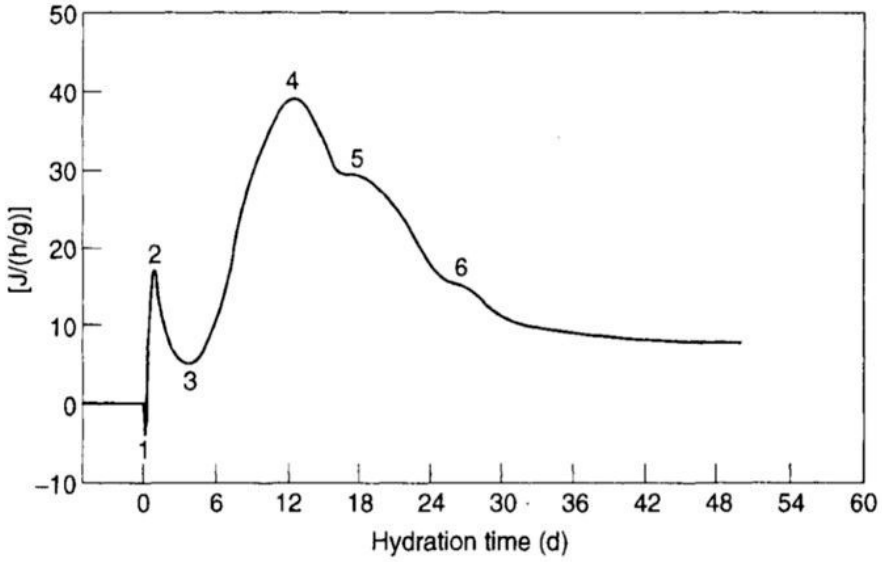

Figure 5. Hydration heat evolution of an OPC vs. hydration time. Step 1: K_2SO_4 dissolution. Step 2: Early-stage period. Step 3: Dormant period. Step 4: Middle-stage period (C-S-H formation). Step 5: AFt formation. Step 6: Aft–AFm conversion. Reprinted with permission from [1].

4. Setting of OPC

The setting time is the elapsed time from the addition of water to a cement mixture until it reaches a specified level of rigidity (measured by a specific technical procedure). Setting consists of the conversion of a plastic cementitious paste into a set material, which is no longer deformable [1]. This conversion is gradual and continuous, and the setting time is usually quantified by measuring the penetration resistance by means of a Vicat needle (i.e., ASTM C191-21) [82]. In general, setting is usually preceded by a stiffening of the paste (with an increment in the material viscosity, even if the mixture does not lose its plastic behavior). Furthermore, it is important to distinguish between the term "setting" and "hardening". Hardening occurs after the setting step, and it refers to an increase in terms of mechanical properties (i.e., Young's modulus, strength, and hardness) until the material reaches the final value of these ones.

4.1. Mechanism of Setting

The mechanism of setting passes through the contact between water and the OPC grains. Quite soon, formed particles of cement undertake flocculation during mixing, thus increasing the viscosity of the cement. After a few minutes of mixing, only coarse (approx. 10 μm) and fine (approx. 3 μm) particles are dispersed in the medium (i.e., water), with the formation of few aggregates of coarse particles, which entrap a fraction of the water. During the induction (dormant) period (i.e., hydration of C_3S), flocculation is reversible, and aggregates are re-dispersed by remixing the paste. Once the acceleration period starts, C-S-H starts to precipitate from the AFt phase, and it is registered as an increment in the fraction of hydrated material and a consequent decrement in the volume of liquid. Thus, particles agglomerate with the fine ones. The principal hydrated compound is C-S-H, which is strongly 3D-connected, and agglomeration cannot be re-dispersed by simply mixing. By continuing with the hydration process, the quantity of products continues growing and the bonding between particles strengthens, thus providing a gradual increment in the strength of the cementitious set paste. Figure 6 reports the mechanism of the flocculation of the cement paste [83,84].

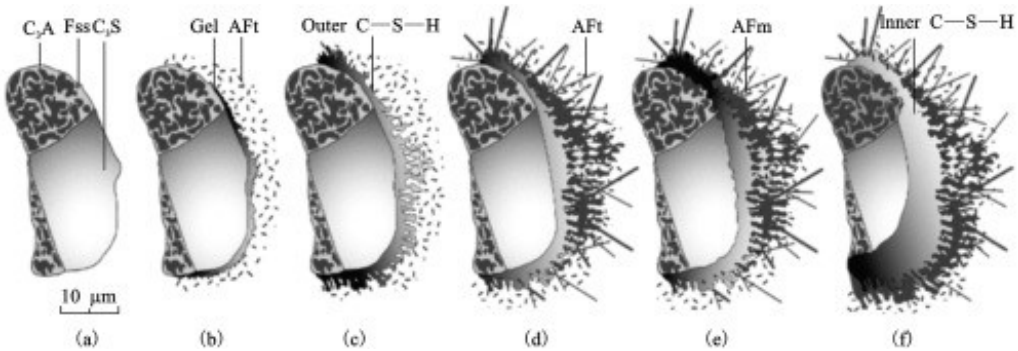

Figure 6. Image showing the mechanism of flocculation: (**a**) unhydrated section of polymineralic grain (scale of interstitial phase is slightly exaggerated), (**b**) after 10 min, (**c**) after 10 h, (**d**) after 18 h, (**e**) after 1-3 days, (**f**) after 14 days [83].

4.2. Flash Setting vs. False Setting

At this point, it is mandatory to clarify the difference existing between flash setting and false setting. "Flash setting" consists of the fast loss of plasticity of the pastes once mixed with water, thus reducing the effective time of workability of the cement. Such a rapid transformation is caused by the increment in the early reactions involving aluminate and ferrite chemical species, with the production of plates of AFm all over the material, and the release of a high heat of hydration [65]. The meshwork of AFm plates, responsible for minimizing the possibilities of remixing, is overcome by the more compact coatings of AFt phases formed in presence of gypsum, which is a set regulator. Gypsum dissolves in

water, releasing Ca^{2+} and SO_4^{2-} ions. As previously discussed, the quantity of hydrated C_3A and C_4AF in the pre-induction period is reduced, with the consequent formation of the AFt phase during hydration. This AFt phase precipitates at the surface of the cement grain forming a microcrystalline layer. In this way, the flowability and plasticity of the cement paste is maintained until the formation of the hydrated phases, such as C-S-H that induces the "normal setting".

On the other hand, the term "false setting" refers to the formation of secondary gypsum (i.e., calcium sulphate dehydrated) crystals, in the presence of either a very low amount or an absence of C_3A. In this case, this "false setting" is caused by the interlocking of gypsum crystals, and, simply, intensive mixing can restore the plasticity of the mixture. "False setting" is typical for cements containing high concentrations of either K_2O (i.e., precipitation of $K_2Ca(SO_4)_2$), or C_3A (i.e., excessive formation of the AFt phase).

5. Pore Structure in OPC

5.1. Type of Porosities

In hardened cementitious materials, there are four types of pores, namely: gel pores, capillary pores, hallow-shell pores, and entrapped/entrained air voids [85].

Gel pores (size of approx. a few nm) form within the hydrated phases at the interface between the cement grains with the liquid. Due to their small size and the great affinity between gel surfaces with water molecules, the movement of the liquid water within gel pores does not contribute to the cement paste permeability.

Capillary pores (sized between a few nm to a few microns) form from the spaces in the fresh paste initially filled with water. During hardening, such spaces evolve into either interconnected channels or gel-pore interconnected cavities. Capillary pores are highly irregular, and their presence is due to the volume of water used during the hydration process. Since a high *w*/*c* ratio causes high porosity in the hardened paste, capillary pores are typically formed in formulation with *w*/*c* ratios larger than 0.42 [86].

Hollow-shell pores (size of several microns) are closed, ink-bottle pores that form within the void spaces at the borders of cement grains as they move back during hydration, whose shape is a relict of the cement particles.

Entrapped air voids form during mixing due to the high viscosity of the paste. These voids are irregular and typically isolated from each other. Entrained air voids, instead, are intentionally formed during the cement mixing. These voids are uniformly distributed, spherical in shape, and not interconnected with each other [86].

5.2. Type of Water

The introduction of water within the initial mixing of the cementitious paste allows for the formation of hardened cement through hydration. Moreover, there are three different categories of water: (i) chemically bound water, (ii) physically bound (gel) water, and (iii) free (evaporable) water. Chemically bound water forms a solid cementitious paste. Gel water, instead, is the water physically bound to C-S-H gel. The sum of chemically and physically bound water provides the minimum amount of water to fully hydrate a given quantity of cement, thus fixing the *w*/*c* ratio at 0.42 [86,87]. Lastly, free (evaporable) water is the water contained in the capillary network of pores.

5.3. Bleeding Phenomenon Involcing the Action of Water in Cementitious Paste

Bleeding is a particular type of sedimentation, where a definite volume of mixing water remains separated at the surface of the cementitious matrix. The implication of this is the reduction in the final volume of the hardened paste soon after the placement, resulting in interparticle distance reduction and variation in the effective *w*/*c* ratio, which results being smaller than the initial one. The properties of cement paste showing bleeding are defined by the sedimentation rate and the volume of bleeding water, calculated as the difference between the initial mixing water and the water effectively inside the cement.

The bleeding-induced effect increases with the *w*/*c* ratio, thus for a high *w*/*c* ratio, it is mandatory to add anti-settling agents. Examples of anti-settling agents are bentonite, hydro-soluble polymers, and inorganic salts. Such anti-settling agents act in different ways, namely: adsorbing large quantities of water to preserve the homogeneity of the slurry (i.e., bentonite) [88], increasing the cohesiveness between cement hydrates and the viscosity of the medium (i.e., hydro-soluble polymers) [89], or entrapping water within weak-bounded hydroxide structures formed within the slurry volumes (i.e., inorganic salts) [90].

6. Future Perspective in the Use of Recycled (Waste) Materials in Cementitious Matrices

The use of recycled (waste) materials in the construction sector can achieve significant benefits in terms of both environmental preservation (i.e., saving natural resources, reducing the amount of greenhouse gas emissions and energy consumption) and processing costs. Quite recently, several studies report the use of waste materials as a substitute counterpart for the aggregate fraction in the preparations of concrete and mortar, trying to either maintain or (better) improve the final mechanical properties. The use of materials deriving from the demolition of structures (i.e., construction and demolition waste, CDW) is one of the major studied waste substrates that attract the interests of scientific literature. For example, Villoria Sàez et al. [91] proposed to examine and compare CDW generation in all EU member states in correlation with their respective national construction businesses, gross domestic product, and capital, together with an assessment of the policy framework and CDW recovery performance of each member state against the recovery target of the waste framework directive. The results show that Austria, Germany, the Netherlands, Belgium, and France are the highest CDW producers, whereas Croatia, Slovenia, Slovakia, Poland, Portugal, and Spain were the lowest ones. Liikanen et al. [92], instead, evaluated the role played by raw materials for wood-plastic composites (WPC) to achieve the CDW recovery target in Finland. Specifically, the objective of this analysis was to assess the environmental impacts of WPC production using specific CDW fractions (i.e., wood, plastic, gypsum board, and mineral wool) as raw materials, and to compare these impacts with the traditional situation in which these CDW fractions are treated by conventional methods. The results indicate that, compared with the traditional situation, the environmental impacts of CDW management can be reduced when CDW fractions are used in WPC production. Moreover, Coelho et al. [93] evaluated the economic implications of traditional demolition and selective demolition, analyzing a case study in Portugal. Several scenarios are considered, based on possible waste management options, some of which favor selective demolition over a conventional one. By considering the Italian situation, Borghi et al. [94] applied life-cycle assessment (LCA) methodology to assess the environmental performance of construction and demolition materials in the current context of the management of the Lombardy region, identifying critical aspects related to the management system of non-hazardous CDW and possible actions for improvement (e.g., increment and refinement of the quality of the recycled aggregate). Moving away from Europe, Contreras et al. [95] analyzed a case study in Brazil where CDW was used to produce new building materials, replacing the natural aggregate fraction to produce novel (sustainable) bricks showing superior average compression strength than standard bricks. This finding shows that it is possible to produce low-cost bricks with excellent physical properties using CDW as an aggregate and lime/cement as an additive. Ossa et al. [96] conducted a study regarding the use of recycled CDW aggregate to create asphalt mixtures for urban roads. Numerous tests were conducted to evaluate the susceptibility of the asphalt concrete samples to moisture damage and plastic deformation (typical for this specific application). The results indicate that it is possible to use CDW aggregates (up to 20%) to pave urban roads. In a recent study by Coelho et al. [97], the technological, economic, and environmental aspects related to operational CDW recycling facilities that produce medium- to high-quality recycled concrete aggregates have been reported (for details please refers to [97]). Interestingly, Marzouk et al. [98] evaluate the impact of two

alternatives for CDW management, namely: either recycling or disposal. The results show that CDW recycling leads to significant reductions in emissions, energy consumption, global warming potential, and conserves landfill space compared to the disposal of waste in landfills. Gálvez-Martos et al. [99] summarize the key principles and best practices for CDW management across the entire construction value chain. Systematic implementation of these best practices could dramatically improve resource efficiency and reduce environmental impacts: reducing waste generation, minimizing transportation impacts and reuse/recycling, improving the quality of secondary materials, and optimizing the environmental performance of treatment methods. Lastly, Jesus et al. [100] studied the behavior of cementitious renderings incorporating very fine recycled aggregates from two types of CDW: recycled concrete aggregate (RCA, smaller one) and mixed recycled aggregate (MRA). Results pointed out that the modified mortars in most of the tests showed superior performance than the reference mortar (without CDW). An interesting and alternative use of recycled waste materials in concrete is reported by Ma et al. [101], who propose a novel route for utilizing recycled coarse aggregate in high-quality recycled manufactured sand, and the use of such high-quality sand to prepare recycled mortar with good mechanical strength and durability, thus further increasing the value of recycling concrete waste.

Furthermore, the use of alternative aggregates, besides those deriving from CDW, is another frequently discussed topic from the literature [102]. Among the possible recycled substrates, plastic waste that would be destined for landfills is attractive not only from the sustainability and economy viewpoint, but also for their very peculiar mechanical properties [103]. In this context, the literature proposes a multitude of different polymeric substrates to be exploited as aggregate fractions, fillers or fibers in the preparation of novel (green) functional concrete, such as polyethylene terephthalate (PET) [104–112], poly vinyl chloride (PVC) [113,114], high density polyethylene (HDPE) [115], shredded and recycled plastic waste [102,116,117], expanded polystyrene foams (EPS) [118,119], polycarbonate [120], or polyurethane foams [121,122]. Even if the use of polymeric materials in concrete often leads to a decrease in the mechanical properties due to several factors, such as the poor adherence between the plastic aggregates and the cementitious matrix, and the granular characteristics of the polymeric waste (which in most cases is not sufficient to achieve the optimum packing leading to the minimum of porosity) [117], the use of plastic waste can also be properly exploited for the introduction of some specific properties, unconventional for ordinary concrete. Currently, there is a growing interest in the use of recycled rubber (mostly derived from tire waste) in concrete as a partial replacement of the aggregate fraction [16,17,123,124]. In fact, the addition of rubber particles into concrete can introduce novel properties in cement, such as a limitation of the water absorption and a consequent improvement against corrosion, a reduction in noise propagation, and a further improvement in fire resistance [125]. Furthermore, in the literature, the use of rubber concrete in non-structural applications is also suggested [14,126]. In this context, an important point that should be considered is that the introduction of rubber fragments as aggregate fraction in cementitious matrices significantly affects the final mechanical properties of the cement/concrete in a proportional way in respect to the rubber content [16,17].

7. Conclusions

Due to their remarkable mechanical properties, cementitious materials are among the most largely exploited substrates used by the construction industry for building cities, and linking them with highways, roads, and bridges. However, even if cement is a well-consolidated material, its chemistry remains very complex and not obvious. In order to try to improve the comprehension of the chemistry of cement, the present document has been organized into five parts.

Part I (Paragraph 2) describes the manufacture process for obtaining ordinary Portland cement (OPC).

Part II (Paragraph 3) provides information on the chemical composition of OPC, which is a mixture of different inorganic oxides (i.e., mainly CaO, SiO_2, Al_2O_3, Fe_2O_3), and deepens the understanding of the hydration mechanisms of every component forming the cement. Particular attention has been dedicated towards the evolution of the chemical composition in the cement system with time, after the reaction with water.

Part III (Paragraph 4) is focused on the mechanism of setting, fundamental for improving structural integrity in the final material.

Part IV (Paragraph 5) deals with the different types of porosities available in a cement. Additionally, a paragraph dedicated to the pivotal role of water in driving the pore formation has been provided.

Part V (Paragraph 6) reports the recent findings of the alternative use of recycled (waste) materials in cementitious matrices, thus highlighting the future trends for the sustainable development of cementitious formulations.

Based on the analysis of the literature, the following important statements can be delivered*:*

(1) Water plays a fundamental role in the evolution of the cement matrix. Since the hydration process consists of a series of different chemical reactions involving the main components of the cement powder with water, the reaction products deriving from the hydration mechanism strongly affect the final chemical composition of the cement.

(2) During the setting time, there is a conversion from a plastic paste towards a set material, whereas the mechanical properties of the formulation are defined after the hardening step.

(3) It is possible to distinguish between three different types of water: (i) chemically bound water, (ii) physically bound (gel) water, and (iii) free (evaporable) water.

(4) Every type of water influences the porosity of the cement, and consequently the mechanical performance.

(5) It is possible to use recycled (waste) materials and reuse them in cementitious matrices to form sustainable (advanced) cementitious composites.

(6) The recent interest in smart inorganic materials for advanced technological applications opens the possibility of using cement as a matrix for novel nanoscopic composites with improved properties (e.g., self-healing and health-monitoring materials).

Author Contributions: Conceptualization, L.L. and R.N.; writing—original draft preparation, L.L.; writing—review and editing, L.L. and R.N. All authors have read and agreed to the published version of the manuscript.

Funding: This research received no external funding.

Institutional Review Board Statement: Not applicable.

Informed Consent Statement: Not applicable.

Data Availability Statement: Not applicable.

Acknowledgments: Authors would like to thank M. Pavese, and E. Chiavazzo (Polytechnic of Torino, Italy) for fruitful discussions, and D. Burlon, and M.L. Aghemo for their precious help.

Conflicts of Interest: The authors declare no conflicts of interest.

References

1. Odler, I. 6-Hydration, Setting and Hardening of Portland Cement. In *Lea's Chemistry of Cement and Concrete*, 4th ed.; Hewlett, P.C., Ed.; Butterworth-Heinemann: Oxford, UK, 1998; pp. 241–297, ISBN 978-0-7506-6256-7.
2. Cadix, A.; James, S. Chapter 5-Cementing Additives. In *Fluid Chemistry, Drilling and Completion*; Wang, Q., Ed.; Gulf Professional Publishing: Dhahram, Saudi Arabia, 2022; pp. 187–254, ISBN 978-0-12-822721-3.
3. Ludwig, H.-M.; Zhang, W. Research Review of Cement Clinker Chemistry. *Cem. Concr. Res.* **2015**, *78*, 24–37. https://doi.org/10.1016/j.cemconres.2015.05.018.

4. Krishnya, S.; Elakneswaran, Y.; Yoda, Y. Proposing a Three-Phase Model for Predicting the Mechanical Properties of Mortar and Concrete. *Mater. Today Commun.* **2021**, *29*, 102858. https://doi.org/10.1016/j.mtcomm.2021.102858.
5. Gagg, C.R. Cement and Concrete as an Engineering Material: An Historic Appraisal and Case Study Analysis. *Eng. Fail. Anal.* **2014**, *40*, 114–140. https://doi.org/10.1016/j.engfailanal.2014.02.004.
6. Liu, M.; Xia, Y.; Zhao, Y.; Cao, Z. Immobilization of Cu (II), Ni (II) and Zn (II) in Silica Fume Blended Portland Cement: Role of Silica Fume. *Constr. Build. Mater.* **2022**, *341*, 127772. https://doi.org/10.1016/j.conbuildmat.2022.127772.
7. Xue, C. Performance and Mechanisms of Stimulated Self-Healing in Cement-Based Composites Exposed to Saline Environments. *Cem. Concr. Compos.* **2022**, *129*, 104470. https://doi.org/10.1016/j.cemconcomp.2022.104470.
8. Papaioannou, S.; Amenta, M.; Kilikoglou, V.; Gournis, D.; Karatasios, I. Synthesis and Integration of Cement-Based Capsules Modified with Sodium Silicate for Developing Self-Healing Cements. *Constr. Build. Mater.* **2022**, *316*, 125803. https://doi.org/10.1016/j.conbuildmat.2021.125803.
9. Sun, M.; Liew, R.J.Y.; Zhang, M.-H.; Li, W. Development of Cement-Based Strain Sensor for Health Monitoring of Ultra High Strength Concrete. *Constr. Build. Mater.* **2014**, *65*, 630–637. https://doi.org/10.1016/j.conbuildmat.2014.04.105.
10. Cassese, P.; Rainieri, C.; Occhiuzzi, A. Applications of Cement-Based Smart Composites to Civil Structural Health Monitoring: A Review. *Appl. Sci.* **2021**, *11*, 8530. https://doi.org/10.3390/app11188530.
11. Lavagna, L.; Bartoli, M.; Suarez-Riera, D.; Cagliero, D.; Musso, S.; Pavese, M. Oxidation of Carbon Nanotubes for Improving the Mechanical and Electrical Properties of Oil-Well Cement-Based Composites. *ACS Appl. Nano Mater.* **2022**, *5*, 6671–6678. https://doi.org/10.1021/acsanm.2c00706.
12. Jia, L.; Shi, C.; Pan, X.; Zhang, J.; Wu, L. Effects of Inorganic Surface Treatment on Water Permeability of Cement-Based Materials. *Cem. Concr. Compos.* **2016**, *67*, 85–92. https://doi.org/10.1016/j.cemconcomp.2016.01.002.
13. Lavagna, L.; Burlon, D.; Nisticò, R.; Brancato, V.; Frazzica, A.; Pavese, M.; Chiavazzo, E. Cementitious Composite Materials for Thermal Energy Storage Applications: A Preliminary Characterization and Theoretical Analysis. *Sci. Rep.* **2020**, *10*, 12833. https://doi.org/10.1038/s41598-020-69502-0.
14. Nisticò, R.; Lavagna, L.; Boot, E.A.; Ivanchenko, P.; Lorusso, M.; Bosia, F.; Pugno, N.M.; D'Angelo, D.; Pavese, M. Improving Rubber Concrete Strength and Toughness by Plasma-induced End-of-life Tire Rubber Surface Modification. *Plasma Process Polym.* **2021**, *18*, 2100081. https://doi.org/10.1002/ppap.202100081.
15. Siddika, A.; Mamun, M.A.A.; Alyousef, R.; Amran, Y.H.M.; Aslani, F.; Alabduljabbar, H. Properties and Utilizations of Waste Tire Rubber in Concrete: A Review. *Constr. Build. Mater.* **2019**, *224*, 711–731. https://doi.org/10.1016/j.conbuildmat.2019.07.108.
16. Lavagna, L.; Nisticò, R.; Sarasso, M.; Pavese, M. An Analytical Mini-Review on the Compression Strength of Rubberized Concrete as a Function of the Amount of Recycled Tires Crumb Rubber. *Materials* **2020**, *13*, 1234. https://doi.org/10.3390/ma13051234.
17. Roychand, R.; Gravina, R.J.; Zhuge, Y.; Ma, X.; Youssf, O.; Mills, J.E. A Comprehensive Review on the Mechanical Properties of Waste Tire Rubber Concrete. *Constr. Build. Mater.* **2020**, *237*, 117651. https://doi.org/10.1016/j.conbuildmat.2019.117651.
18. Chen, Y.K.; Sun, Y.; Wang, K.Q.; Kuang, W.Y.; Yan, S.R.; Wang, Z.H.; Lee, H.S. Utilization of Bio-Waste Eggshell Powder as a Potential Filler Material for Cement: Analyses of Zeta Potential, Hydration and Sustainability. *Constr. Build. Mater.* **2022**, *325*, 126220. https://doi.org/10.1016/j.conbuildmat.2021.126220.
19. Nisticò, R.; Lavagna, L.; Versaci, D.; Ivanchenko, P.; Benzi, P. Chitosan and Its Char as Fillers in Cement-Base Composites: A Case Study. *Boletín De La Soc. Española De Cerámica Y Vidr.* **2020**, *59*, 186–192. https://doi.org/10.1016/j.bsecv.2019.10.002.
20. Suarez-Riera, D.; Merlo, A.; Lavagna, L.; Nisticò, R.; Pavese, M. Mechanical Properties of Mortar Containing Recycled Acanthocardia Tuberculata Seashells as Aggregate Partial Replacement. *Boletín De La Soc. Española De Cerámica Y Vidr.* **2021**, *60*, 206–210. https://doi.org/10.1016/j.bsecv.2020.03.011.
21. Cement|OEC. Available online: https://oec.world/en/profile/hs/cement (accessed on 12 December 2022).
22. Xu, Z.; Guo, Z.; Zhao, Y.; Li, S.; Luo, X.; Chen, G.; Liu, C.; Gao, J. Hydration of Blended Cement with High-Volume Slag and Nano-Silica. *J. Build. Eng.* **2023**, *64*, 105657. https://doi.org/10.1016/j.jobe.2022.105657.
23. Balachandran, C.; Muñoz, J.F.; Peethamparan, S.; Arnold, T.S. Alkali -Silica Reaction and Its Dynamic Relationship with Cement Pore Solution in Highly Reactive Systems. *Constr. Build. Mater.* **2023**, *362*, 129702. https://doi.org/10.1016/j.conbuildmat.2022.129702.
24. Xia, Y.; Liu, M.; Zhao, Y.; Chi, X.; Guo, J.; Du, D.; Du, J. Hydration Mechanism and Phase Assemblage of Blended Cement with Iron-Rich Sewage Sludge Ash. *J. Build. Eng.* **2023**, *63*, 105579. https://doi.org/10.1016/j.jobe.2022.105579.
25. Zheng, X.; Liu, K.; Gao, S.; Wang, F.; Wu, Z. Effect of Pozzolanic Reaction of Zeolite on Its Internal Curing Performance in Cement-Based Materials. *J. Build. Eng.* **2023**, *63*, 105503. https://doi.org/10.1016/j.jobe.2022.105503.
26. Deng, X.; Guo, H.; Tan, H.; Zhang, J.; Zheng, Z.; Li, M.; Chen, P.; He, X.; Yang, J.; Wang, J. Comparison on Early Hydration of Portland Cement and Sulphoaluminate Cement in the Presence of Nano Ettringite. *Constr. Build. Mater.* **2022**, *360*, 129516. https://doi.org/10.1016/j.conbuildmat.2022.129516.
27. Fang, Z.; Wang, C.; Hu, H.; Zhou, S.; Luo, Y. Effect of Electrical Field on the Stability of Hydration Products of Cement Paste in Different Liquid Media. *Constr. Build. Mater.* **2022**, *359*, 129489. https://doi.org/10.1016/j.conbuildmat.2022.129489.
28. Hou, J.; He, X.; Ni, X. Hydration Mechanism and Thermodynamic Simulation of Ecological Ternary Cements Containing Phosphogypsum. *Mater. Today Commun.* **2022**, *33*, 104621. https://doi.org/10.1016/j.mtcomm.2022.104621.
29. Zhang, Y.; Yang, W.; Wang, Y.; Gong, Z.; Zhang, K. Molecular Dynamics Simulation of C-S-H Corrosion in Chloride Environment. *Mater. Today Commun.* **2022**, *33*, 104568. https://doi.org/10.1016/j.mtcomm.2022.104568.

30. Aretxabaleta, X.M.; López-Zorrilla, J.; Labbez, C.; Etxebarria, I.; Manzano, H. A Potential C-S-H Nucleation Mechanism: Atomistic Simulations of the Portlandite to C-S-H Transformation. *Cem. Concr. Res.* **2022**, *162*, 106965. https://doi.org/10.1016/j.cemconres.2022.106965.
31. Yi, Y.; Ma, W.; Sidike, A.; Ma, Z.; Fang, M.; Lin, Y.; Bai, S.; Chen, Y. Synergistic Effect of Hydration and Carbonation of Ladle Furnace Aslag on Cementitious Substances. *Sci. Rep.* **2022**, *12*, 14526. https://doi.org/10.1038/s41598-022-18215-7.
32. Zunino, F.; Dhandapani, Y.; Ben Haha, M.; Skibsted, J.; Joseph, S.; Krishnan, S.; Parashar, A.; Juenger, M.C.G.; Hanein, T.; Bernal, S.A.; et al. Hydration and Mixture Design of Calcined Clay Blended Cements: Review by the RILEM TC 282-CCL. *Mater. Struct.* **2022**, *55*, 234. https://doi.org/10.1617/s11527-022-02060-1.
33. Maruyama, I.; Sugimoto, H.; Umeki, S.; Kurihara, R. Effect of Fineness of Cement on Drying Shrinkage. *Cem. Concr. Res.* **2022**, *161*, 106961. https://doi.org/10.1016/j.cemconres.2022.106961.
34. Li, H.-W.; Wang, R.; Wei, M.-W.; Lei, N.-Z.; Sun, H.-X.; Fan, J.-J. Mechanical Properties and Hydration Mechanism of High-Volume Ultra-Fine Iron Ore Tailings Cementitious Materials. *Constr. Build. Mater.* **2022**, *353*, 129100. https://doi.org/10.1016/j.conbuildmat.2022.129100.
35. Ma, Y.; Li, W.; Jin, M.; Liu, J.; Zhang, J.; Huang, J.; Lu, C.; Zeng, H.; Wang, J.; Zhao, H.; et al. Influences of Leaching on the Composition, Structure and Morphology of Calcium Silicate Hydrate (C–S–H) with Different Ca/Si Ratios. *J. Build. Eng.* **2022**, *58*, 105017. https://doi.org/10.1016/j.jobe.2022.105017.
36. Liu, R.; Fang, B.; Zhang, G.; Guo, J.; Yang, Y. Investigation of Sodium Alginate as a Candidate Retarder of Magnesium Phosphate Cement: Hydration Properties and Its Retarding Mechanism. *Ceram. Int.* **2022**, *48*, 30846–30852. https://doi.org/10.1016/j.ceramint.2022.07.038.
37. Wang, X.; Zhao, Q.; Zhang, S.; Lu, N. Pre-Curing Time Effect on Reactive Powder Concrete Impact Resistance. *AIP Adv.* **2022**, *12*, 105025. https://doi.org/10.1063/5.0104255.
38. Li, B.; Tang, Z.; Huo, B.; Liu, Z.; Cheng, Y.; Ding, B.; Zhang, P. The Early Age Hydration Products and Mechanical Properties of Cement Paste Containing GBFS under Steam Curing Condition. *Buildings* **2022**, *12*, 1746. https://doi.org/10.3390/buildings12101746.
39. Yan, Z.; Zhang, H.; Zhu, Y. Hydration Kinetics of Sulfoaluminate Cement with Different Water/Cement Ratios as Grouting Material Used for Coal Mines. *Mag. Concr. Res.* **2022**, *74*, 1056–1064. https://doi.org/10.1680/jmacr.21.00129.
40. Dong, P.; Allahverdi, A.; Andrei, C.M.; Bassim, N.D. The Effects of Nano-Silica on Early-Age Hydration Reactions of Nano Portland Cement. *Cem. Concr. Compos.* **2022**, *133*, 104698. https://doi.org/10.1016/j.cemconcomp.2022.104698.
41. Ma, J.; Liu, X.; Yu, Z.; Shi, H.; Wu, Q.; Shen, X. Effects of Limestone Powder on the Early Hydration of Tricalcium Aluminate. *J. Therm. Anal. Calorim.* **2022**, *147*, 10351–10362. https://doi.org/10.1007/s10973-022-11287-7.
42. Achternbosch, M.; Bräutigam, K.R.; Hartlieb, N.; Kupsch, C.; Richers, U.; Stemmermann, P.; Gleis, M. *Heavy Metals in Cement and Concrete Resulting from the Co-Incineration of Wastes in Cement Kilns with Regard to the Legitimacy of Waste Utilisation*; *Forschungszentrum Karlsruhe GmbH,* Karlsruhe Germany,2003.
43. de Queiroz Lamas, W.; Palau, J.C.F.; de Camargo, J.R. Waste Materials Co-Processing in Cement Industry: Ecological Efficiency of Waste Reuse. *Renew. Sustain. Energy Rev.* **2013**, *19*, 200–207. https://doi.org/10.1016/j.rser.2012.11.015.
44. Hwidi, R.S.; Tengku Izhar, T.N.; Mohd Saad, F.N. Characterization of Limestone as Raw Material to Hydrated Lime. *E3S Web Conf.* **2018**, *34*, 02042. https://doi.org/10.1051/e3sconf/20183402042.
45. Schumacher, G.; Juniper, L. 15-Coal Utilisation in the Cement and Concrete Industries. In *The Coal Handbook: Towards Cleaner Production*; Osborne, D., Ed.; Woodhead Publishing: Sawston, UK, 2013; Volume 2, pp. 387–426, ISBN 978-1-78242-116-0.
46. Lea, F.M.; Mason, T.O. *Cement-Extraction and Processing*; Encyclopædia Britannica, Inc.: 2019.
47. Whittaker, M.; Dubina, E.; Plank, J.; Black, L. The Effects of Prehydration on Cement Performance. In Proceedings of the 30th Cement and Concrete Science Conference, Birmingham, UK, 13–15 September 2010.
48. Nisticò, R. A Comprehensive Study on the Applications of Clays into Advanced Technologies, with a Particular Attention on Biomedicine and Environmental Remediation. *Inorganics* **2022**, *10*, 40. https://doi.org/10.3390/inorganics10030040.
49. Nisticò, R. The Importance of Surfaces and Interfaces in Clays for Water Remediation Processes. *Surf. Topogr. Metrol. Prop.* **2018**, *6*, 043001. https://doi.org/10.1088/2051-672X/aaed09.
50. Powers, T.C.; Brownyard, T.L. Studies of the Physical Properties of Hardened Portland Cement Paste. *ACI J. Proc.* **1946**, *43*, 249–336. https://doi.org/10.14359/15301.
51. Alesiani, M.; Pirazzoli, I.; Maraviglia, B. Factors Affecting Early-Age Hydration of Ordinary Portland Cement Studied by NMR: Fineness, Water-to-Cement Ratio and Curing Temperature. *Appl. Magn. Reson.* **2007**, *32*, 385–394. https://doi.org/10.1007/s00723-007-0019-y.
52. Soler, J.M. Thermodynamic Description of the Solubility of C-S-H Gels in Hydrated Portland Cement Literature Review; Posiva Oy, Toeoeloenkatu 4, FIN-00100 Helsinki, Finland, **2007**. http://www.posiva.fi/publications/WR2007-88web.pdf
53. Wang, L.; Yang, H.Q.; Zhou, S.H.; Chen, E.; Tang, S.W. Hydration, Mechanical Property and C-S-H Structure of Early-Strength Low-Heat Cement-Based Materials. *Mater. Lett.* **2018**, *217*, 151–154. https://doi.org/10.1016/j.matlet.2018.01.077.
54. de Jong, J.G.M.; Stein, H.N.; Stevels, J.M. Hydration of Tricalcium Silicate. *J. Appl. Chem.* **2007**, *17*, 246–250. https://doi.org/10.1002/jctb.5010170902.
55. Cuesta, A.; Zea-Garcia, J.D.; Londono-Zuluaga, D.; De La Torre, A.G.; Santacruz, I.; Vallcorba, O.; Dapiaggi, M.; Sanfélix, S.G.; Aranda, M.A.G. Multiscale Understanding of Tricalcium Silicate Hydration Reactions. *Sci. Rep.* **2018**, *8*, 8544. https://doi.org/10.1038/s41598-018-26943-y.

56. Thomas, J.J.; Ghazizadeh, S.; Masoero, E. Kinetic Mechanisms and Activation Energies for Hydration of Standard and Highly Reactive Forms of β-Dicalcium Silicate (C2S). *Cem. Concr. Res.* **2017**, *100*, 322–328. https://doi.org/10.1016/j.cemconres.2017.06.001.
57. Park, S.M.; Jang, J.G.; Son, H.M.; Lee, H.K. Stable Conversion of Metastable Hydrates in Calcium Aluminate Cement by Early Carbonation Curing. *J. CO2 Util.* **2017**, *21*, 224–226. https://doi.org/10.1016/j.jcou.2017.07.002.
58. *Lea's Chemistry of Cement and Concrete*, 5th ed.; Lea, F.M., Hewlett, P.C., Liška, M., Butterworth-Heinemann.: Oxford Cambridge United Kingdom 2019; ISBN 978-0-08-100773-0.
59. Taylor, H.F.W.; Famy, C.; Scrivener, K.L. Delayed Ettringite Formation. *Cem. Concr. Res.* **2001**, *31*, 683–693. https://doi.org/10.1016/S0008-8846(01)00466-5.
60. Marchon, D.; Flatt, R.J. 8-Mechanisms of Cement Hydration. In *Science and Technology of Concrete Admixtures*; Aïtcin, P.-C., Flatt, R.J., Eds.; Woodhead Publishing: Sawston, UK, 2016; pp. 129–145, ISBN 978-0-08-100693-1.
61. Meller, N.; Hall, C.; Crawshaw, J. ESEM Evidence for Through-Solution Transport during Brownmillerite Hydration. *J. Mater. Sci.* **2004**, *39*, 6611–6614. https://doi.org/10.1023/B:JMSC.0000044904.51813.74.
62. Rose, J.; Bénard, A.; El Mrabet, S.; Masion, A.; Moulin, I.; Briois, V.; Olivi, L.; Bottero, J.Y. Evolution of Iron Speciation during Hydration of C4AF. *Waste Manag.* **2006**, *26*, 720–724. https://doi.org/10.1016/j.wasman.2006.01.021.
63. Flick, E.W. *Handbook of Adhesive Raw Materials*; William Andrew: 1989; ISBN 0-8155-1185-X.
64. Nicoleau, L.; Schreiner, E.; Nonat, A. Ion-Specific Effects Influencing the Dissolution of Tricalcium Silicate. *Cem. Concr. Res.* **2014**, *59*, 118–138. https://doi.org/10.1016/j.cemconres.2014.02.006.
65. Scherer, G.W.; Zhang, J.; Thomas, J.J. Nucleation and Growth Models for Hydration of Cement. *Cem. Concr. Res.* **2012**, *42*, 982–993. https://doi.org/10.1016/j.cemconres.2012.03.019.
66. Scrivener, K.L.; Juilland, P.; Monteiro, P.J.M. Advances in Understanding Hydration of Portland Cement. *Cem. Concr. Res.* **2015**, *78*, 38–56. https://doi.org/10.1016/j.cemconres.2015.05.025.
67. Double, D.D.; Hellawell, A.; Perry, S.J.; Hirsch, P.B. The Hydration of Portland Cement. *Proc. R. Soc. London. A. Math. Phys. Sci.* **1978**, *359*, 435–451. https://doi.org/10.1098/rspa.1978.0050.
68. Meredith, P.; Donald, A.M.; Luke, K. Pre-Induction and Induction Hydration of Tricalcium Silicate: An Environmental Scanning Electron Microscopy Study. *J. Mater. Sci.* **1995**, *30*, 1921–1930. https://doi.org/10.1007/BF00353014.
69. Thomas, N.L.; Double, D.D. Calcium and Silicon Concentrations in Solution during the Early Hydration of Portland Cement and Tricalcium Silicate. *Cem. Concr. Res.* **1981**, *11*, 675–687. https://doi.org/10.1016/0008-8846(81)90026-0.
70. Jiahui, P.; Jianxin, Z.; Jindong, Q. The Mechanism of the Formation and Transformation of Ettringite. *J. Wuhan Univ. Technol. - Mater. Sci. Ed.* **2006**, *21*, 158–161. https://doi.org/10.1007/BF02840908.
71. El-Didamony, H.; Sharara, A.M.; Helmy, I.M.; Abd El-Aleem, S. Hydration Characteristics of β-C2S in the Presence of Some Accelerators. *Cem. Concr. Res.* **1996**, *26*, 1179–1187. https://doi.org/10.1016/0008-8846(96)00103-2.
72. Jennings, H.M.; Pratt, P.L. An Experimental Argument for the Existence of a Protective Membrane Surrounding Portland Cement during the Induction Period. *Cem. Concr. Res.* **1979**, *9*, 501–506. https://doi.org/10.1016/0008-8846(79)90048-6.
73. Jia, F.; Yao, Y.; Wang, J. Influence and Mechanism Research of Hydration Heat Inhibitor on Low-Heat Portland Cement. *Front. Mater.* **2021**, *8*, 697380. https://doi.org/10.3389/fmats.2021.697380.
74. Ouzia, A.R.C.W.C. *Modeling the Kinetics of the Main Peak and Later Age of Alite Hydration*; EPFL: Lausanne, Switzerland, 2019; p. 288. https://doi.org/10.5075/epfl-thesis-9499.
75. Juilland, P.; Nicoleau, L.; Arvidson, R.S.; Gallucci, E. Advances in Dissolution Understanding and Their Implications for Cement Hydration. *RILEM Tech. Lett.* **2017**, *2*, 90–98. https://doi.org/10.21809/rilemtechlett.2017.47.
76. Tennis, P.D.; Jennings, H.M. Model for Two Types of Calcium Silicate Hydrate in the Microstructure of Portland Cement Pastes. *Cem. Concr. Res.* **2000**, *30*, 855–863. https://doi.org/10.1016/S0008-8846(00)00257-X.
77. Sakalli, Y.; Trettin, R. Investigation of C3S Hydration by Environmental Scanning Electron Microscope. *J. Microsc.* **2015**, *259*, 53–58. https://doi.org/10.1111/jmi.12247.
78. Zhutovsky, S.; Kovler, K. Chemical Shrinkage of High-Strength/High-Performance Cementitious Materials. *International Review of Chemical Engineering* **2018**, *10*, 110–118.
79. Bazzoni, A.; Ma, S.; Wang, Q.; Shen, X.; Cantoni, M.; Scrivener, K.L. The Effect of Magnesium and Zinc Ions on the Hydration Kinetics of C3S. *J. Am. Ceram. Soc.* **2014**, *97*, 3684–3693. https://doi.org/10.1111/jace.13156.
80. Barnes, P.; Bensted, J. *Structure and Performance of Cements*; CRC Press: Boca Raton, FL, USA, 2002; ISBN 0-429-17842-5.
81. Ben Haha, M.; Winnefeld, F.; Pisch, A. Advances in Understanding Ye'elimite-Rich Cements. *Cem. Concr. Res.* **2019**, *123*, 105778. https://doi.org/10.1016/j.cemconres.2019.105778.
82. C01 Committee. *Test Methods for Time of Setting of Hydraulic Cement by Vicat Needle*; ASTM International: West Conshohocken, PA, USA, 2006.
83. Yuan, Q.; Liu, Z.; Zheng, K.; Ma, C. Chapter 2-Inorganic Cementing Materials. In *Civil Engineering Materials*; Yuan, Q., Liu, Z., Zheng, K., Ma, C., Eds.; Elsevier: Amsterdam, The Netherlands, 2021; pp. 17–57, ISBN 978-0-12-822865-4.
84. Taylor, H.F.W. 4 Properties of Portland Clinker and Cement. In *Cement Chemistry*, Thomas Telford Publishing: London, United Kingdom, 1997; pp. 89–112.
85. Wang, L.; Jin, M.; Wu, Y.; Zhou, Y.; Tang, S. Hydration, Shrinkage, Pore Structure and Fractal Dimension of Silica Fume Modified Low Heat Portland Cement-Based Materials. *Constr. Build. Mater.* **2021**, *272*, 121952. https://doi.org/10.1016/j.conbuildmat.2020.121952.

86. Aïtcin, P.-C.; Lessard, J.-M. 8-The Composition and Design of High-Strength Concrete and Ultrahigh-Strength Concrete. In *Developments in the Formulation and Reinforcement of Concrete*, 2nd ed.; Mindess, S., Ed.; Woodhead Publishing: Sawston, UK, 2019; pp. 171–192 ISBN 978-0-08-102616-8.
87. Ley-Hernandez, A.M.; Lapeyre, J.; Cook, R.; Kumar, A.; Feys, D. Elucidating the Effect of Water-To-Cement Ratio on the Hydration Mechanisms of Cement. *ACS Omega* **2018**, *3*, 5092–5105. https://doi.org/10.1021/acsomega.8b00097.
88. Mesboua, N.; Benyounes, K.; Benmounah, A. Study of the Impact of Bentonite on the Physico-Mechanical and Flow Properties of Cement Grout. *Cogent Eng.* **2018**, *5*, 1446252. https://doi.org/10.1080/23311916.2018.1446252.
89. Nguyen, D.D.; Devlin, L.P.; Koshy, P.; Sorrell, C.C. Impact of Water-Soluble Cellulose Ethers on Polymer-Modified Mortars. *J. Mater. Sci.* **2014**, *49*, 923–951. https://doi.org/10.1007/s10853-013-7732-8.
90. Xie, N.; Dang, Y.; Shi, X. New Insights into How MgCl2 Deteriorates Portland Cement Concrete. *Cem. Concr. Res.* **2019**, *120*, 244–255. https://doi.org/10.1016/j.cemconres.2019.03.026.
91. Villoria Sáez, P.; Osmani, M. A Diagnosis of Construction and Demolition Waste Generation and Recovery Practice in the European Union. *J. Clean. Prod.* **2019**, *241*, 118400. https://doi.org/10.1016/j.jclepro.2019.118400.
92. Liikanen, M.; Grönman, K.; Deviatkin, I.; Havukainen, J.; Hyvärinen, M.; Kärki, T.; Varis, J.; Soukka, R.; Horttanainen, M. Construction and Demolition Waste as a Raw Material for Wood Polymer Composites—Assessment of Environmental Impacts. *J. Clean. Prod.* **2019**, *225*, 716–727. https://doi.org/10.1016/j.jclepro.2019.03.348.
93. Coelho, A.; de Brito, J. Economic Analysis of Conventional versus Selective Demolition—A Case Study. *Resour. Conserv. Recycl.* **2011**, *55*, 382–392. https://doi.org/10.1016/j.resconrec.2010.11.003.
94. Borghi, G.; Pantini, S.; Rigamonti, L. Life Cycle Assessment of Non-Hazardous Construction and Demolition Waste (CDW) Management in Lombardy Region (Italy). *J. Clean. Prod.* **2018**, *184*, 815–825. https://doi.org/10.1016/j.jclepro.2018.02.287.
95. Contreras, M.; Teixeira, S.R.; Lucas, M.C.; Lima, L.C.N.; Cardoso, D.S.L.; da Silva, G.A.C.; Gregório, G.C.; de Souza, A.E.; dos Santos, A. Recycling of Construction and Demolition Waste for Producing New Construction Material (Brazil Case-Study). *Constr. Build. Mater.* **2016**, *123*, 594–600. https://doi.org/10.1016/j.conbuildmat.2016.07.044.
96. Ossa, A.; García, J.L.; Botero, E. Use of Recycled Construction and Demolition Waste (CDW) Aggregates: A Sustainable Alternative for the Pavement Construction Industry. *J. Clean. Prod.* **2016**, *135*, 379–386. https://doi.org/10.1016/j.jclepro.2016.06.088.
97. Coelho, A.; De Brito, J. 9-Preparation of Concrete Aggregates from Construction and Demolition Waste (CDW). In *Handbook of Recycled Concrete and Demolition Waste*; Pacheco-Torgal, F., Tam, V.W.Y., Labrincha, J.A., Ding, Y., de Brito, J., Eds.; Woodhead Publishing: Sawston, UK, 2013; pp. 210–245, ISBN 978-0-85709-682-1.
98. Marzouk, M.; Azab, S. Environmental and Economic Impact Assessment of Construction and Demolition Waste Disposal Using System Dynamics. *Resour. Conserv. Recycl.* **2014**, *82*, 41–49. https://doi.org/10.1016/j.resconrec.2013.10.015.
99. Gálvez-Martos, J.-L.; Styles, D.; Schoenberger, H.; Zeschmar-Lahl, B. Construction and Demolition Waste Best Management Practice in Europe. *Resour. Conserv. Recycl.* **2018**, *136*, 166–178. https://doi.org/10.1016/j.resconrec.2018.04.016.
100. Jesus, S.; Maia, C.; Brazão Farinha, C.; de Brito, J.; Veiga, R. Rendering Mortars with Incorporation of Very Fine Aggregates from Construction and Demolition Waste. *Constr. Build. Mater.* **2019**, *229*, 116844. https://doi.org/10.1016/j.conbuildmat.2019.116844.
101. Ma, Z.; Shen, J.; Wang, C.; Wu, H. Characterization of Sustainable Mortar Containing High-Quality Recycled Manufactured Sand Crushed from Recycled Coarse Aggregate. *Cem. Concr. Compos.* **2022**, *132*, 104629. https://doi.org/10.1016/j.cemconcomp.2022.104629.
102. Saikia, N.; de Brito, J. Use of Plastic Waste as Aggregate in Cement Mortar and Concrete Preparation: A Review. *Constr. Build. Mater.* **2012**, *34*, 385–401. https://doi.org/10.1016/j.conbuildmat.2012.02.066.
103. El Bitouri, Y.; Perrin, D. Compressive and Flexural Strengths of Mortars Containing ABS and WEEE Based Plastic Aggregates. *Polymers* **2022**, *14*, 3914. https://doi.org/10.3390/polym14183914.
104. Albano, C.; Camacho, N.; Hernández, M.; Matheus, A.; Gutiérrez, A. Influence of Content and Particle Size of Waste Pet Bottles on Concrete Behavior at Different w/c Ratios. *Waste Manag.* **2009**, *29*, 2707–2716. https://doi.org/10.1016/j.wasman.2009.05.007.
105. Choi, Y.W.; Moon, D.J.; Kim, Y.J.; Lachemi, M. Characteristics of Mortar and Concrete Containing Fine Aggregate Manufactured from Recycled Waste Polyethylene Terephthalate Bottles. *Constr. Build. Mater.* **2009**, *23*, 2829–2835. https://doi.org/10.1016/j.conbuildmat.2009.02.036.
106. Choi, Y.-W.; Moon, D.-J.; Chung, J.-S.; Cho, S.-K. Effects of Waste PET Bottles Aggregate on the Properties of Concrete. *Cem. Concr. Res.* **2005**, *35*, 776–781. https://doi.org/10.1016/j.cemconres.2004.05.014.
107. Kim, S.B.; Yi, N.H.; Kim, H.Y.; Kim, J.-H.J.; Song, Y.-C. Material and Structural Performance Evaluation of Recycled PET Fiber Reinforced Concrete. *Cem. Concr. Compos.* **2010**, *32*, 232–240. https://doi.org/10.1016/j.cemconcomp.2009.11.002.
108. Marzouk, O.Y.; Dheilly, R.M.; Queneudec, M. Valorization of Post-Consumer Waste Plastic in Cementitious Concrete Composites. *Waste Manag.* **2007**, *27*, 310–318. https://doi.org/10.1016/j.wasman.2006.03.012.
109. Silva, D.A.; Betioli, A.M.; Gleize, P.J.P.; Roman, H.R.; Gómez, L.A.; Ribeiro, J.L.D. Degradation of Recycled PET Fibers in Portland Cement-Based Materials. *Cem. Concr. Res.* **2005**, *35*, 1741–1746. https://doi.org/10.1016/j.cemconres.2004.10.040.
110. Yesilata, B.; Isıker, Y.; Turgut, P. Thermal Insulation Enhancement in Concretes by Adding Waste PET and Rubber Pieces. *Constr. Build. Mater.* **2009**, *23*, 1878–1882. https://doi.org/10.1016/j.conbuildmat.2008.09.014.
111. Akçaözoğlu, S.; Atiş, C.D.; Akçaözoğlu, K. An Investigation on the Use of Shredded Waste PET Bottles as Aggregate in Lightweight Concrete. *Waste Manag.* **2010**, *30*, 285–290. https://doi.org/10.1016/j.wasman.2009.09.033.

112. Nisticò, R. Polyethylene Terephthalate (PET) in the Packaging Industry. *Polym. Test.* **2020**, *90*, 106707. https://doi.org/10.1016/j.polymertesting.2020.106707.
113. Kou, S.C.; Lee, G.; Poon, C.S.; Lai, W.L. Properties of Lightweight Aggregate Concrete Prepared with PVC Granules Derived from Scraped PVC Pipes. *Waste Manag.* **2009**, *29*, 621–628. https://doi.org/10.1016/j.wasman.2008.06.014.
114. Merlo, A.; Lavagna, L.; Suarez-Riera, D.; Pavese, M. Mechanical Properties of Mortar Containing Waste Plastic (PVC) as Aggregate Partial Replacement. *Case Stud. Constr. Mater.* **2020**, *13*, e00467. https://doi.org/10.1016/j.cscm.2020.e00467.
115. Naik, T.R.; Singh, S.S.; Huber, C.O.; Brodersen, B.S. Use of Post-Consumer Waste Plastics in Cement-Based Composites. *Cem. Concr. Res.* **1996**, *26*, 1489–1492. https://doi.org/10.1016/0008-8846(96)00135-4.
116. Ismail, Z.Z.; AL-Hashmi, E.A. Use of Waste Plastic in Concrete Mixture as Aggregate Replacement. *Waste Manag.* **2008**, *28*, 2041–2047. https://doi.org/10.1016/j.wasman.2007.08.023.
117. Merlo, A.; Lavagna, L.; Suarez-Riera, D.; Pavese, M. Recycling of WEEE Plastics Waste in Mortar: The Effects on Mechanical Properties. *Recycling* **2021**, *6*, 70. https://doi.org/10.3390/recycling6040070.
118. Kan, A.; Demirboğa, R. A Novel Material for Lightweight Concrete Production. *Cem. Concr. Compos.* **2009**, *31*, 489–495. https://doi.org/10.1016/j.cemconcomp.2009.05.002.
119. Kan, A.; Demirboğa, R. A New Technique of Processing for Waste-Expanded Polystyrene Foams as Aggregates. *J. Mater. Process. Technol.* **2009**, *209*, 2994–3000. https://doi.org/10.1016/j.jmatprotec.2008.07.017.
120. Hannawi, K.; Kamali-Bernard, S.; Prince, W. Physical and Mechanical Properties of Mortars Containing PET and PC Waste Aggregates. *Waste Manag.* **2010**, *30*, 2312–2320. https://doi.org/10.1016/j.wasman.2010.03.028.
121. Mounanga, P.; Gbongbon, W.; Poullain, P.; Turcry, P. Proportioning and Characterization of Lightweight Concrete Mixtures Made with Rigid Polyurethane Foam Wastes. *Cem. Concr. Compos.* **2008**, *30*, 806–814. https://doi.org/10.1016/j.cemconcomp.2008.06.007.
122. Ben Fraj, A.; Kismi, M.; Mounanga, P. Valorization of Coarse Rigid Polyurethane Foam Waste in Lightweight Aggregate Concrete. *Constr. Build. Mater.* **2010**, *24*, 1069–1077. https://doi.org/10.1016/j.conbuildmat.2009.11.010.
123. Sgobba, S.; Borsa, M.; Molfetta, M.; Marano, G.C. Mechanical Performance and Medium-Term Degradation of Rubberised Concrete. *Constr. Build. Mater.* **2015**, *98*, 820–831. https://doi.org/10.1016/j.conbuildmat.2015.07.095.
124. Nacif, G.L.; Panzera, T.H.; Strecker, K.; Christoforo, A.L.; Paine, K. Investigations on Cementitious Composites Based on Rubber Particle Waste Additions. *Mater. Res.* **2012**, *16*, 259–268. https://doi.org/10.1590/S1516-14392012005000177.
125. Asdrubali, F.; D'Alessandro, F.; Schiavoni, S.; Baldinelli, G. *Lightweight Screeds Made of Concrete and Recycled Polymers: Acoustic, Thermal, Mechanical and Chemical Characterization*; *Forum Acusticum*, 2011: Aalborg, Denmark; pp. 821–826.
126. Abaza, O.A.; Shtayeh, S.M. Crumbed Rubber for Non-Structural Portland Cement Concrete Applications. *Eng. Sci.* **2010**, *37*, 214-225.